공학석사 학위논문

Modeling of the effective field dependent mobility for the random discrete dopant simulation

랜덤 불연속 도펀트의 시뮬레이션에 대해 이펙티브 필드에 의존하는 이동도 모델 수립

2018 년 2 월

서울대학교 대학원

전기정보공학부

김 대 원

Modeling of the effective field dependent mobility for the random discrete dopant simulation

랜덤 불연속 도펀트의 시뮬레이션에 대해

이펙티브 필드에 의존하는 이동도 모델 수립

지도 교수 박 영 준

이 논문을 공학석사 학위논문으로 제출함

2018 년 2 월

서울대학교 대학원

전기정보공학부

김 대 원

김대원의 공학석사 학위논문을 인준함

2018 년 2 월

위 원 장 박 병 국 (인)

부위원장 박 영 준 (인)

위 원 이 종 호 (인)

Abstract

In the thesis, an ‘effective field dependent’ mobility model, which can be applied to the random discrete dopants (RDD) simulation of the current variation, is proposed. In order to evaluate the characteristics of the silicon devices considering the RDD, the proper electrostatic and mobility model should be used simultaneously. To deal with the discrete dopants, the electrostatic effect can be modeled by the density gradient (DG) methods, but the appropriate mobility model for the RDD simulation has not been fully exploited.

The conventional doping-dependent mobility model such as the Masetti model has been widely used because the device sizes are relatively larger than the varying range of the doping concentration. However, if one applies this Masetti model to the RDD simulation, it leads to incorrectly high terminal currents, since the mobility values of each mesh are determined abnormally. By the doping-dependent nature of the Masetti model, the meshes with the extremely high doping concentrations (representing the individual dopants) have very low mobility values. But, the remaining ‘intrinsic’ meshes have the maximum mobility, and it leads to the incorrect high terminal currents. In order to reproduce the ‘target’ current in the RDD simulation, the proper mobility model for the RDD simulation should be available.

First, a new quantity called ‘mobility field’ is defined in each mesh. The mobility field is derived from the definition of the renowned effective field of the Takagi *et al*., considering the analogy between the inversion layer in the MOS surfaces and the vicinity of the discrete dopants. This new mobility field still

includes the physical consistency with the conventional effective field which determines the mobility of the devices. The consistency is confirmed using the MOS simulation. Second, the formula of the mobility value in each mesh is established using this mobility field, and the model parameters is found to make the resultant currents of the RDD simulation reproduce the correct current targets. Using the proposed mobility model and the model parameters, the terminal currents of the RDD simulation successfully reproduce the target currents with the linear error rate of < 1% for the wide range of doping concentrations and temperatures simultaneously.

The determined model parameters have intriguing properties. The coefficients in the mobility formula have the linear and the exponential dependence to the inverse of the temperature, respectively. The exponents in the formula have the values near 1/3 and 3/2, respectively. These quantities are related to the conventional surface mobility degradation models such as the Lombardi model, which includes the linearity to $1/T$ and 1/3-dependence to the transverse electric fields. It can be considered that the same physical scattering effects are governed near the surface channel region and the discrete dopants.

Keyword: Random discrete dopants, TCAD simulation, mobility model, effective field, field-dependent mobility

Student Number: 2016-20870

Table of Contents

List of Tables

List of Figures

Chapter 1. Introduction

1.1. Motivation

As the MOSFET technology has been scaled down to sub-100 nm nodes, the carrier transport associated the randomness and discreteness of the impurity dopants becomes more important. Most of the researches dealing with the random discrete dopants (RDD) have focused on the electrostatic effect in the channel region to predict the variability of the threshold voltage [1-13]. When evaluating the RDD effect in the channel region, the source/drain (S/D) regions may be approximated by the continuous doping profile [10]. This could be successful because of two reasons following: (i) the doping concentration of the S/D regions was 10^2 – 10^3 times higher than that of the channel regions, and (ii) the mobility fluctuation due to the channel RDD affects linearly in the I-V characteristics so it could not affect to the threshold voltage fluctuation which has log-scale properties.

However, in the devices of the recent technology nodes, the RDD effects in the S/D regions should also be considered because of its scaled and limited volume. For example, in the state-of-the-art dynamic random-access memory (DRAM), the number of dopants in the S/D regions is only a few hundreds, which can lead to the increased ON-current fluctuation in addition to the threshold voltage variation caused by the channel RDD [14]. Also, in order to avoid the side effects such as the gate-induced-drain-leakage (GIDL) effects, the doping concentration of the S/D regions for the modern devices is gradually decreasing, so the randomness and discreteness of the dopants in the S/D region should be considered.

The effects of the RDD to the current and threshold voltage of the devices have been modeled and predicted by the technology computer-aided design (TCAD) simulation. In the simulation of the threshold voltage variation due to the channel RDD, the density gradient (DG) method can be applied as a compact model for evaluating the quantum-mechanically corrected electrostatic effects near the discrete dopants [16]. However, in the simulation of the current variation caused by the RDD such as those in the channel and the S/D regions, the conventional doping-dependent mobility model such as the Masetti model is incomplete in predicting both the average and fluctuation in the terminal current value. The mobility model including the impurity scattering to account for the RDD effect has not been fully exploited even though the model is critically important to predict the current and its variation [17-19].

1.2. Outline of the Thesis

In this thesis, an ‘effective field dependent’ mobility model is proposed, which can be generally applied to the RDD simulation of the current variation. First, a new quantity called ‘mobility field’ is defined in each mesh, which is derived from the definition of the renowned effective field [20], considering the analogy between the inversion layer in the MOS surfaces and the vicinity of the discrete dopants. Subsequently, the formula for the mobility value in each mesh is established using the mobility field, and the model parameters is obtained to make the resultant currents of the RDD simulation reproduce the correct current targets. Furthermore, the physical meaning of each term in the mobility formula is explained.

Chapter 2. Simulation Testbed and Problem Analysis

2.1. Test Structure for the Simulation

For developing the mobility model for the RDD effect, the N-type silicon resistors with various doping concentrations having the uniform and continuous impurity profile are generated, as shown in Fig. 2.1a. The dimensions of these resistors are 20 nm × 20 nm × 140 nm to contain enough number of the discrete dopants, and the range of the impurity concentration is set from 10^{17} to 10^{20} cm^{-3}. For each structure, the 'target' terminal currents are obtained for low bias (20 mV) by applying the conventional doping-dependent Masetti mobility model for various temperatures. These 'target' currents can be assumed identical to the empirical results of the actual silicon resistors, since the Masetti model is the empirically fitted formula by the measurement results of the actual silicon for various doping concentrations [21].

For the counterpart simulation containing the 'realistic' RDD instead of the hypothetical continuous doping profile in Fig. 2.1a, the discrete dopants are deployed in the intermediate channel region of each resistor, as shown in Fig. 2.1b. These discrete dopants are distributed in the spatially random manner without any background doping concentration to describe the intrinsic base [22]. The picture of intrinsic base can be considered as realistic description because the individual doping impurities are located within the intrinsic silicon lattice structures. Some authors used the simulation structure with base doping in order to avoid the numerical artifacts, but this structure cannot be realistic because the total number

of dopants could not be maintained. The continuously doped regions are remained at both ends of the resistors to avoid the numerical problems at the contacts. In this procedure, only the samples which contain the number of total dopants in the device same are generated as the counterpart continuous structures. It should be noted that two groups of the simulation structures represent the actual N-type silicon resistors in the different way.

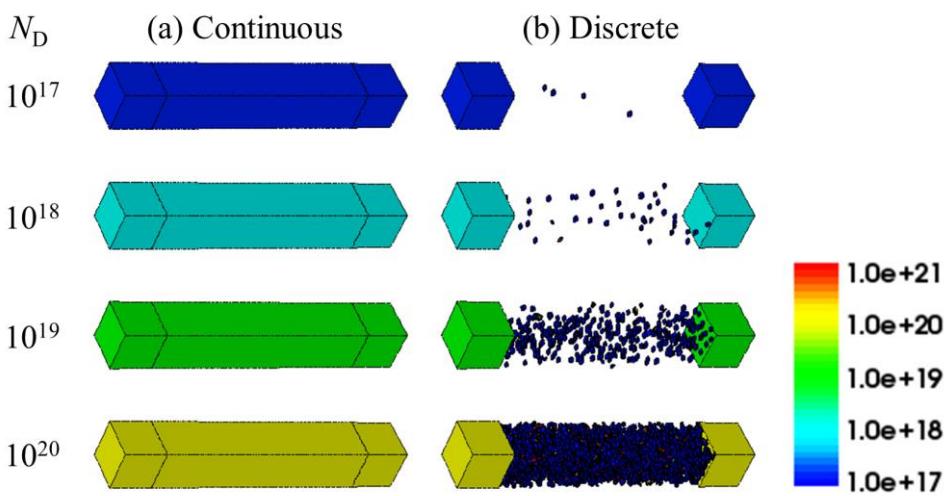

Fig. 2.1. The N-type silicon resistors as the simulation testbed. (a) The resistors with uniform and continuous doping concentration for evaluating the 'target' terminal currents. (b) The resistors with RDD in the intermediate regions. Dots indicate the individual discrete dopants, and the remaining empty space describes the intrinsic region.

2.2. Physical Models and Simulation Conditions

In order to evaluate the terminal currents of two sets of the simulation structures, the electrostatic model and the mobility model are carefully selected. The transport scheme is the drift-diffusion equation. The mesh spacing is set as 1 nm × 1 nm × 1 nm, in order to balance between the accuracy of the simulation results and the computational burden and elapsed time. Therefore, for the RDD structures, the doping concentration of meshes including the single dopants becomes 10^{21} cm^{-3}.

The electrostatic model is based on the Poisson's equation, but the density gradient (DG) method is selected for the quantum mechanical correction for the calculation of the electron density. The DG method is originally invented to describe the quantum mechanical effects in the surface channel of the traditional MOSFET devices [24], but Asenov *et al*. have found out that the DG method can be utilized successfully to describe the electron density in the vicinity of the discrete dopants [16]. The formula of the DG method is integrated in the Poisson's equation as follows;

$$n = N_{\mathrm{C}} F_{1/2}\left(\frac{E_{\mathrm{F},n} - E_{\mathrm{C}} - \Lambda_n}{k_{\mathrm{B}} T_n}\right) \tag{1}$$

$$\Lambda_n = -\frac{\gamma \hbar^2}{6 m_n} \frac{\nabla^2 \sqrt{n}}{\sqrt{n}} \tag{2}$$

where n is the electron density, N_C is the effective density-of-states, $F_{1/2}(x)$ is the Fermi integral of order 1/2 for describing the Fermi statistics, E_C is the conduction band edge, T_n is the lattice temperature, and m_n is the effective mass of the electron, respectively. γ is the fit factor defined in [22].

The drift-diffusion transport scheme needs the appropriate mobility model. In the simulation for this chapter, the conventional doping-dependent mobility model such as the Masetti model is applied [21]. The Masetti model has been established by fitting procedure using enormous empirical data of uniformly doped silicon resistors with various doping concentrations. The formula of the Masetti model is as follows [22];

$$\mu_{dop} = \mu_{min1} \exp\left(-\frac{P_c}{N_A + N_D}\right) + \frac{\mu_{const} - \mu_{min2}}{1 + \left(\frac{N_A + N_D}{C_r}\right)^{\alpha}} - \frac{\mu_1}{1 + \left(\frac{C_s}{N_A + N_D}\right)^{\beta}} \quad (3)$$

where μ_{const} is the lattice phonon scattering mobility term as follows;

$$\mu_{const} = \mu_L \left(\frac{T}{300K}\right)^{-\zeta} \quad (4)$$

and the parameters are extracted as Table 2.1. As in (1), the Masetti mobility model depends on the value of the doping concentration of each mesh, and there is no contribution of the electric field.

Parameter	Electrons	Holes	Unit
μ_{min1}	52.2	44.9	cm^2/Vs
μ_{min2}	52.2	0	cm^2/Vs
μ_1	43.4	29.0	cm^2/Vs
P_c	0	9.23×10^{16}	cm^{-3}
C_r	9.68×10^{16}	2.23×10^{17}	cm^{-3}
C_s	3.43×10^{20}	6.10×10^{20}	cm^{-3}
α	0.680	0.719	1
β	2.0	2.0	1
μ_L	1417	470.5	cm^2/Vs
ζ	2.5	2.2	1

Table 2.1. The model parameters for the Masetti model.

The other miscellaneous simulation conditions are as follows: (i) the Fermi statistics is applied in order to implement the accurate electron density affected by extremely high doping concentrations, (ii) the silicon resistors in Fig 2.1 are covered by the silicon dioxide layer (omitted in Fig 2.1 for clear visualization) in order to set the proper boundary condition in the silicon-dioxide interfaces, (iii) the bandgap narrowing model is neglected in the RDD structure in Fig 2.1b in order to avoid the wrong bandgap around the individual dopants due to the extremely high doping concentration up to 10^{21} cm^{-3}, and (iv) the numerical iteration is conducted by the Newton-Rapson method. The entire simulation is conducted using the Sentaurus of Synopsys, Inc. [22].

2.3. Simulation Results and Problem Analysis

As shown in Fig. 2.2, the average terminal currents of RDD samples are consistently higher than the 'target' currents, even though the same simulation models are maintained such as the DG method and the Masetti mobility model for both the discrete and continuous cases (Fig. 2.1). The deviation of the average terminal currents is due to the mobility model applied to the RDD samples. When

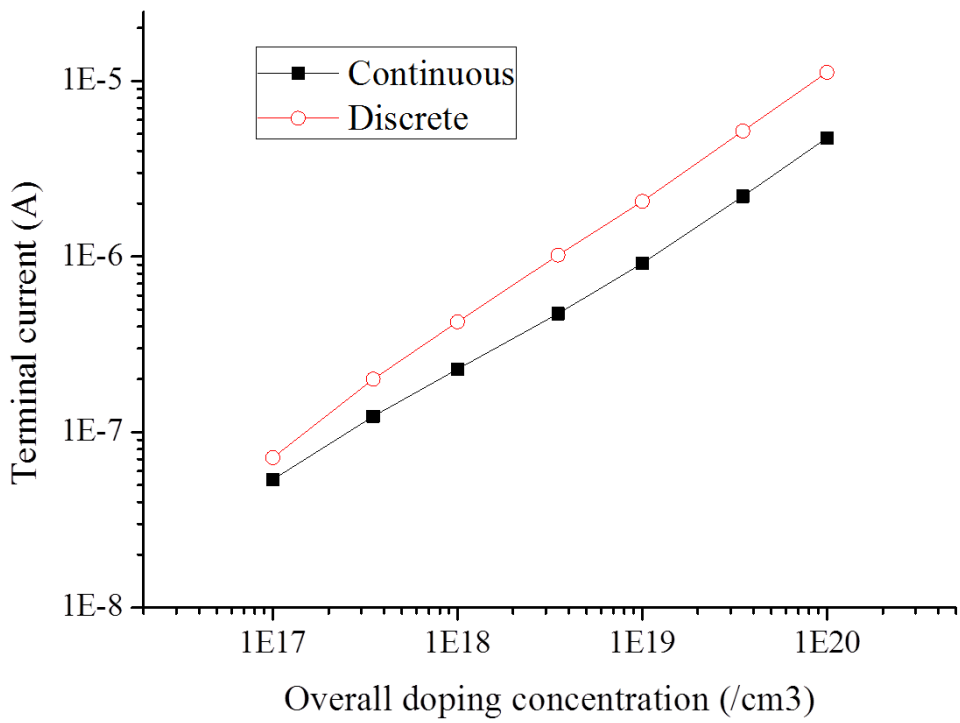

Fig. 2.2. The terminal currents as a function of the overall doping concentration. The conventional Masetti mobility model is applied for both cases. The terminal currents of the discrete samples are the average values over 10 samples.

the Masetti model is applied to the RDD samples, only small number of the single meshes having the dopant atoms are affected by the mobility degradation due to the doping-dependent nature of the model. However, even though the mobility in the meshes having the discrete dopant has very low, the remaining ‘intrinsic’ meshes have the maximum intrinsic mobility values. Since the impurity scattering is a nonlocal phenomenon, the blind application of the mobility model to the mesh in the TCAD framework eventually leads to the incorrect resultant currents. Therefore, the Masetti model is inappropriate to apply to the simulation structures including RDD.

Here, it is worthwhile to notice the following points in consideration of the simple formula for the current density *J*,

$$J = qn\mu E \tag{5}$$

(i) the DG method is able to deal with the electrostatic effect in the vicinity of the discrete dopants properly [16], (ii) the total doping concentration and consequent carrier densities are controlled equally, and (iii) the low terminal voltage suppresses the mobility degradation via the velocity saturation effect. It means that the deviation of the resultant currents in Fig 2.2 is caused by only the inappropriate mobility model, not the electron density or the electric field. Therefore, the proper mobility model for the RDD is critically necessary.

Chapter 3. Model Development

3.1. Definition of the 'Mobility Field'

First, the effective 'mobility field' is defined from the consistency of the effective field and the universal mobility curve related to the traditional MOSFET devices. According to the universal mobility curve in [20], the mobile electrons in the surface channel follow the effective field, which is not the actual normal electric field but defined as

$$E_{\text{eff}} = \frac{Q_d + Q_n / 2}{\varepsilon} \tag{6}$$

where Q_d, Q_n are the areal concentration of the depletion and inversion charge, respectively. The denominator 2 in Q_n indicates that only half of the inversion electron can affect to the entire effective field. The value of the effective field is determined in the entire device, not defined in the each mesh individually. As in the universal mobility curve introduced by Takagi *et al*., the mobility degradation is known to be governed by the surface phonon scattering and the surface roughness scattering, which are due to the Coulomb attraction towards the dielectric-silicon interfaces by the induced charge at the gate electrode, as shown in Fig. 3a.

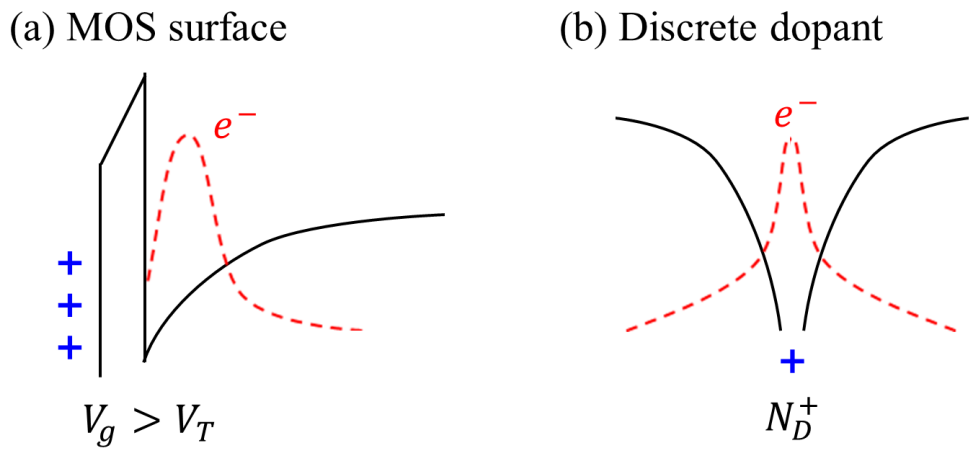

Fig. 3.1. The schematics of the conduction band (black solid) for the MOS surfaces and the discrete dopant, respectively. In both cases, the electrons (red dot) are gathered by the fixed charges, which are (a) the induced one in the gate electrode, or (b) the ionized discrete dopant.

With the similar context as in Fig 3.1, the new quantity of the 'mobility field' is defined as following,

$$E_{\mathrm{mob}}(\boldsymbol{r}) \equiv \frac{q\left(n(\boldsymbol{r})\right)^{2/3}}{2\varepsilon} \tag{7}$$

where $\boldsymbol{r}$ is the coordinate vector of each mesh, $n(\boldsymbol{r})$ is the electron density at the position $\boldsymbol{r}$. The corresponding term of Q_d is not considered since $Q_d << Q_n$ where the electric field is strong enough for the strong inversion and the same

approximation may be applied about the discrete dopants. In the formula (7), the exponent 2/3 is required because the $n(\boldsymbol{r})$ is not the areal charge concentration but the volumetric density from the 3-dimensional mesh-based TCAD simulation. This can be seen as the simple dimension matching, but the verification will be explained later. It should be noted that $n(\boldsymbol{r})$ should be evaluated quantum-mechanically for the physical consistency of $E_{\mathrm{mob}}(\boldsymbol{r})$, since the definition of the original effective field was closely related to the quantum mechanical thickness of the inversion layers [23]. Using the DG method of (1) and (2), the quantum mechanical picture of the carrier concentration is well considered near the discrete dopants [16], as in the semiconductor surface [24].

3.2. Verification of the Consistency between the Effective Field and the Mobility Field

The consistency between the effective field of (6) and the mobility field of (7) is checked by the TCAD simulation of the NMOS device as shown in Fig. 3.2, with various channel doping concentrations, dielectric thicknesses and gate voltages. To obtain the characteristics of the actual devices, the DG method and the conventional mobility models (Masetti, Lombardi, and Canali) are adopted [21,25,26]. These conventional models are designated to fit the empirical I-V characteristics, so the simulation result using these models can be considered as the empirical measurement result.

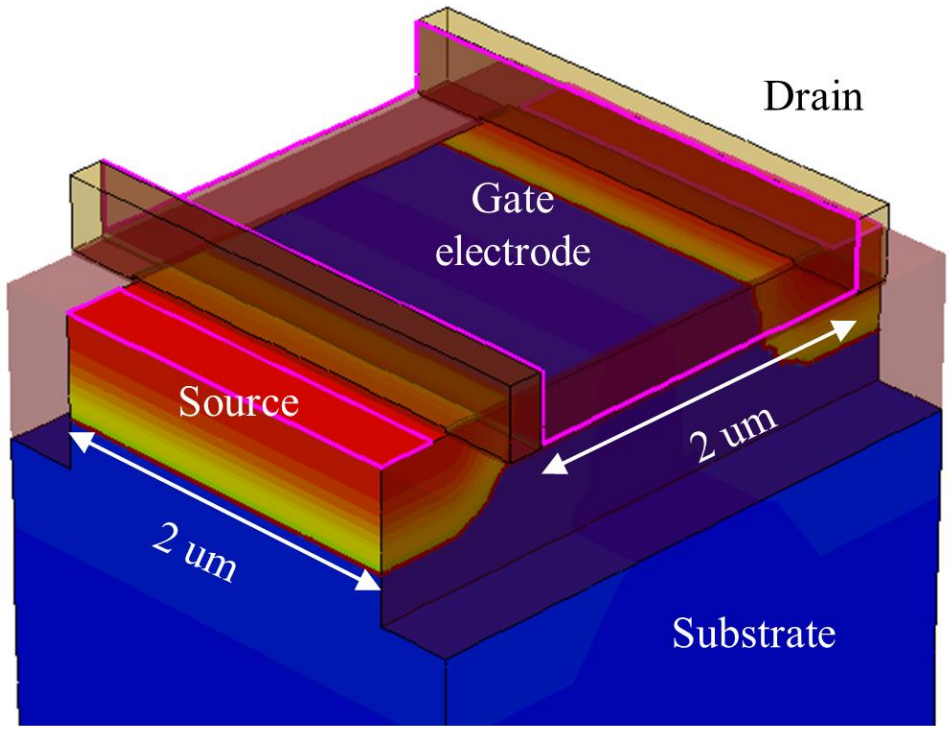

Fig. 3.2. Simulation structure to confirm the consistency between the effective field and the proposed ‘mobility field.’ The width and length of 2 um are enough to minimize the peripheral effects from the S/D regions and the trench oxide.

The Lombardi model is the surface mobility degradation model. The model is designated to calculate the low-field mobility by adding the bulk mobility (extracted by the models such as doping-dependent Masetti model), the acoustic phonon mobility, and the surface roughness mobility degradation. The addition is conducted by the Matthiessen’s rule. The formula of the Lombardi model is as follows [22,25],

$$\frac{1}{\mu_{\text{low}}} = \frac{1}{\mu_{\text{bulk}}} + \frac{D}{\mu_{\text{ac}}} + \frac{D}{\mu_{\text{sr}}} \tag{8}$$

$$\mu_{\text{ac}} = \frac{B}{E_{\perp}} + \frac{C\left(\frac{N_{\text{A}} + N_{\text{D}} + N_2}{N_0}\right)^{\lambda}}{E_{\perp}^{1/3}\left(\frac{T}{300K}\right)^{k}} \tag{9}$$

$$\mu_{\text{sr}} = \left(\frac{\left(E_{\perp} / E_{\text{ref}}\right)^{A}}{\delta} + \frac{E_{\perp}^{3}}{\eta}\right)^{-1} \tag{10}$$

$$D = \exp\left(-\frac{x}{l_{\text{crit}}}\right) \tag{11}$$

The Canali model is the velocity saturation mobility model. The model is based on the Caughey-Thomas model, but verified in wider range of the lattice temperatures, up to 430 K. The formula of the Canali model is as follows [22,26],

$$\mu = \frac{\mu_{\text{low}}}{\left(1 + \left(\frac{\mu_{\text{low}} E}{v_{\text{sat}}}\right)^{\beta}\right)^{1/\beta}} \tag{12}$$

$$\beta = \beta_0 \left(\frac{T}{300K}\right)^{\beta_{\text{exp}}} \tag{13}$$

Every model parameter in the Lombardi model and the Canali model is set to follow the default values provided in the Sentaurus Device User Guide [22].

As a result, the mobility fields at the depth of the maximum electron density show noticeable agreement with the effective fields, which are evaluated by implementing the empirical low-frequency C-V measurement in [20], as shown in Fig. 3.3. In the procedure to evaluate the effective field, 1 kHz of C-V simulation is implemented. Furthermore, since the mobility field is the value defined in every mesh as in (7), only the values in the point of the maximum electron density are examined. By adopting the DG method, the electron density shows the maximum point, which can be considered as the effective location of the inversion electrons.

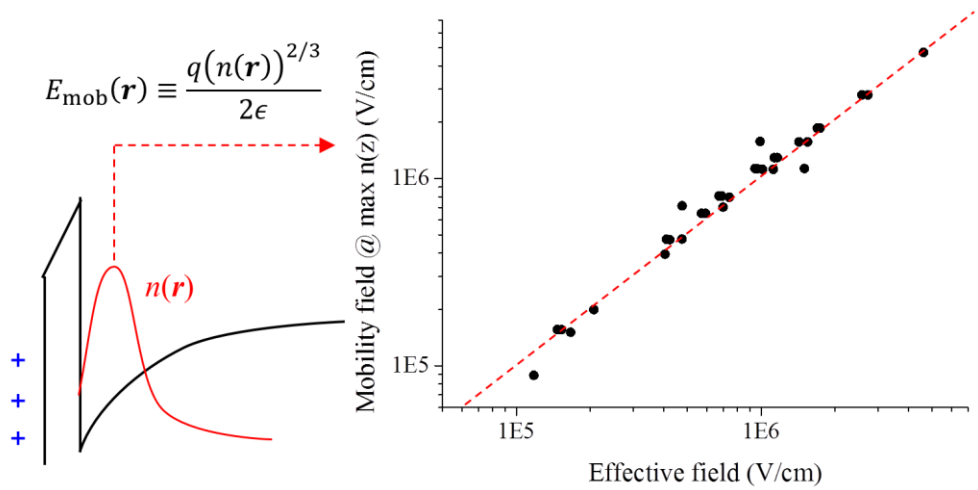

Fig. 3.3. Correlation plot of the effective field and the mobility field for the various channel doping concentration, dielectric thickness, and gate voltage. The effective field is calculated according to the empirical method used in [20], and the mobility field is evaluated at the depth of the maximum electron density.

3.3. Mobility Defined by the Mobility Field

Now the mobility $\mu(\boldsymbol{r})$ is formulated for each mesh using the mobility field $E_{\mathrm{mob}}(\boldsymbol{r})$ defined in (7) and the lattice temperature T as following,

$$\frac{1}{\mu(\boldsymbol{r})} = \frac{1}{\mu_{\mathrm{const}}} + \frac{1}{\mu_{\mathrm{dop}}} \tag{14}$$

where μ_{const} is defined in (4) in the Masetti model, which is the maximum value for the intrinsic silicon (or, for $E_{\mathrm{mob}}(\boldsymbol{r}) \rightarrow 0$), and μ_{dop} is dependent to the mobility field in (7), defined as following,

$$\mu_{\mathrm{dop}} = \frac{B(T)}{E_{\mathrm{mob}}^{\beta}} + \frac{C(T)}{E_{\mathrm{mob}}^{\gamma}} \tag{15}$$

where $B(T)$, $C(T)$, β, and γ are the model parameters determined by the steps to be explained later, It is worthwhile to note that the exponents β, γ are set to invariant to the temperature, besides the coefficients $B(T)$, $C(T)$. Using the proposed mobility model, the terminal currents of the multiple RDD samples are evaluated in the various doping concentrations and temperatures. The form of the formula (14) and (15) is selected for the best fit result of the resultant terminal currents, which will be explained shortly.

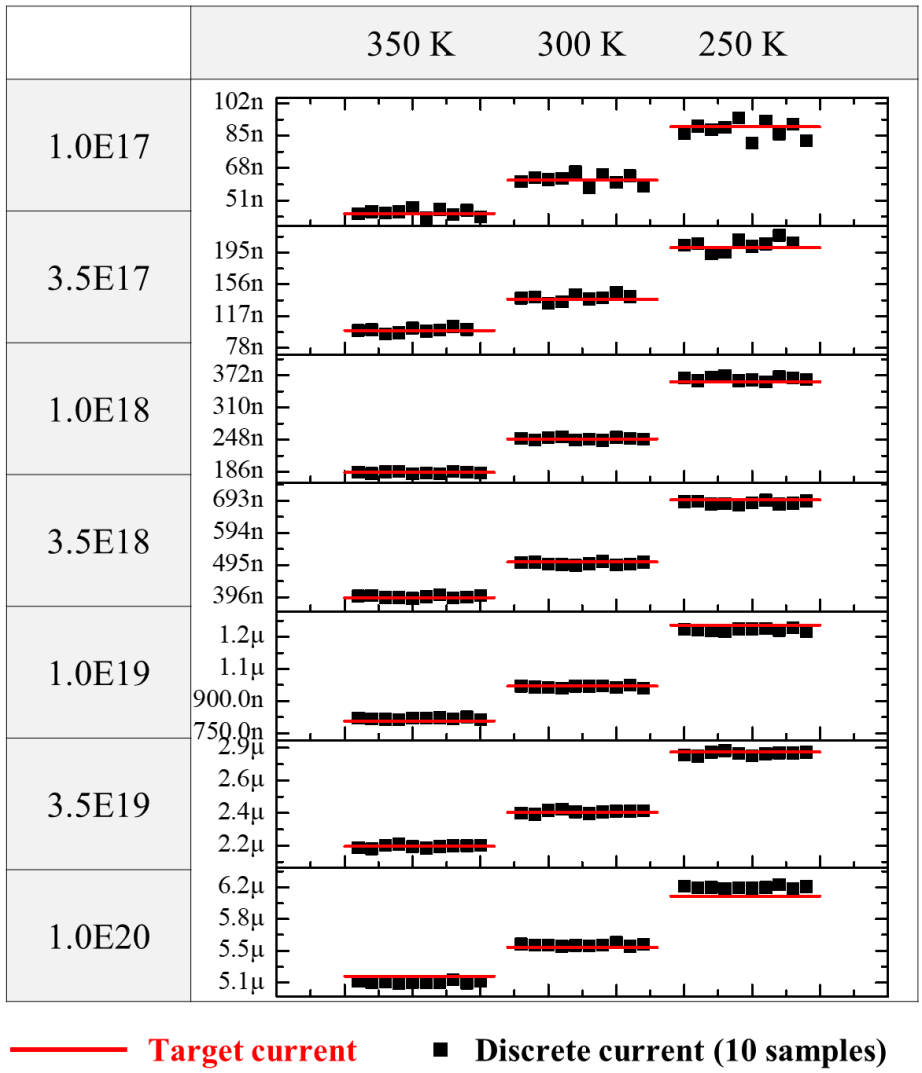

Fig. 3.4. Terminal currents of two simulation cases; (i) the target current from applying the conventional mobility model to the continuous doping, (ii) the discrete currents from applying the proposed mobility model to the 10 RDD samples for each doping concentration.

T	$B(T)$	$C(T)$	β	γ
350 K	7.7530E+3	4.3179E+9		
300 K	8.2617E+3	7.8095E+9	0.32882	1.5331
250 K	9.0035E+3	1.5427E+10		

Table 3.1. The model parameters for the proposed mobility model.

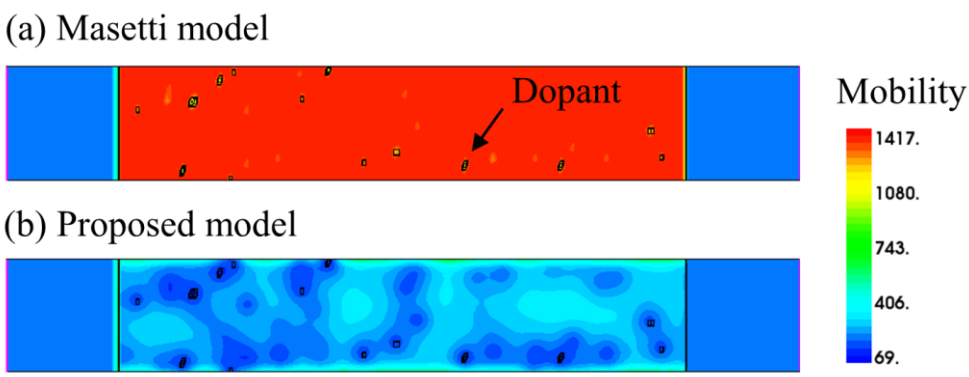

Fig. 3.5. Contour plots of the mobility values on the longitudinal cross-section of an RDD resistor sample of 10^{19} cm^{-3}. (a) Applying the Masetti model leads to the maximum mobility in every mesh except for the discrete dopant positions (black dots). (b) By the proposed mobility model, the nonlocality of the mobility can be described.

As shown in Fig. 3.4 and Table 3.1, the model parameters which make the average terminal currents of the RDD samples reproduce the target currents are extracted. For all cases, the linear error rates of the terminal currents are less than 1%. The resultant mobility profile (Fig. 3.5b) indicates that the nonlocal nature of the Coulomb scattering is considered well as the mobility is dependent on the effective field which includes the nonlocal effect from the RDD by way of $n(\boldsymbol{r})$ which is the solution of the DG method. The mobility profile by the Masetti model (Fig. 3.5a), however, indicates that the simulation artifacts are revealed as mentioned in the Section 2.3, that the small number of the meshes including the single dopants has the low mobility and the remaining intrinsic region has the maximum mobility value.

Intriguingly, the coefficients B, C have dependencies on the inverse temperature $1/T$, as shown in Fig. 3.6, where $B(T)$ is linear, $C(T)$ is exponential to $1/T$, respectively. From this obvious dependency, the general formulae can be constructed,

$$B(T) = (1.095\times10^{6})\times\frac{1}{T} + (4.618\times10^{3}) \tag{16}$$

$$C(T) = \exp\left[(1.108\times10^{3})\times\frac{1}{T} + (1.904\times10^{1})\right] \tag{17}$$

to apply the proposed mobility model to any temperatures. Using (16) and (17) in (15), the proposed mobility model is still applicable in some intermediate temperatures, such as 275 K and 325 K, as shown in Fig. 3.7.

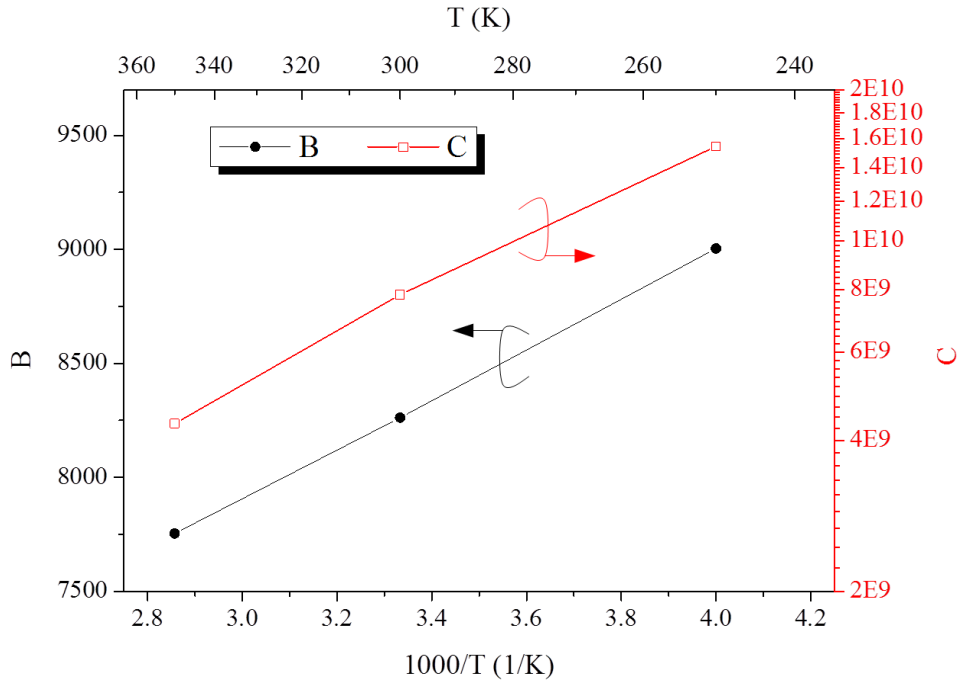

Fig. 3.6. Coefficients $B(T)$, $C(T)$ as a function of the inverse of the temperature. $B(T)$ is linear, and $C(T)$ is exponential to $1/T$.

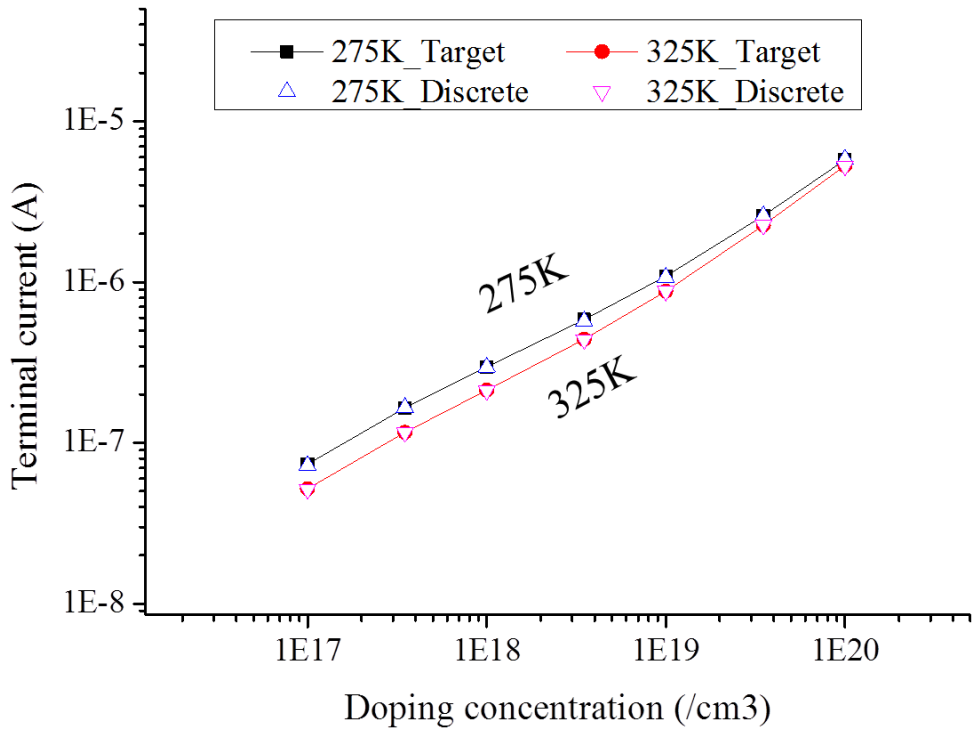

Fig. 3.7. Evaluated terminal currents using the proposed mobility model in intermediate temperatures. Although the model has been established in the specific temperatures (250, 300, 350 K), the general formulae (16) and (17) lead to the resultant currents correctly.

Furthermore, although the proposed model is established in the resistors with the uniform doping concentration, the model should be applicable to any arbitrary doping profiles for the practical uses. To verify the applicability, gradually doped resistor is considered where the doping concentration is varying from 10^{20} cm^{-3} to 10^{18} cm^{-3} in Fig. 3.8. After the same procedure of the dopant randomization, the proposed model is adopted in the multiple RDD samples. As shown in Fig. 3.9, the average terminal currents of the RDD samples are well reproducing the target values for various temperatures. The mobility values are also calculated within the reasonable range corresponding to the doping concentration, as shown in Fig. 3.10. In summary, it has been confirmed that the proposed model can be applied for any cases of the arbitrary temperatures and the realistic nonuniform doping profiles.

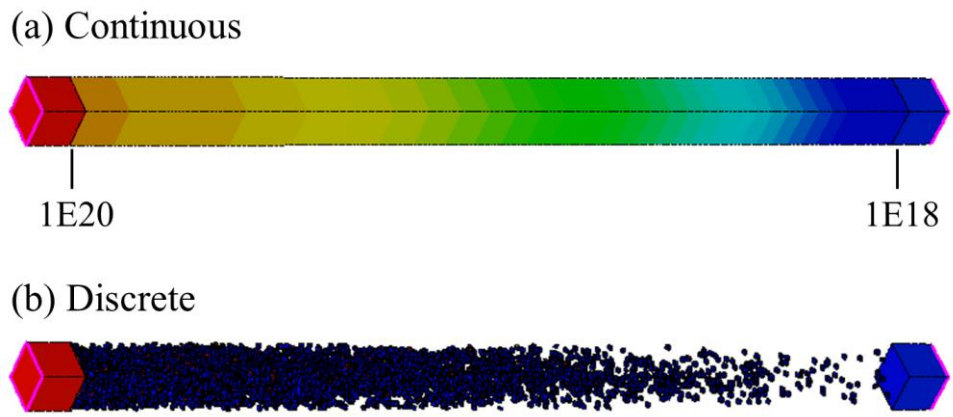

Fig. 3.8. Simulation structures for verifying the applicability of the proposed model in nonuniform doping profile. (a) The continuous and gradual doping resistor, from 10^{20} to 10^{18} cm^{-3}. (b) One of the generated samples including the RDD of the corresponding doping concentration.

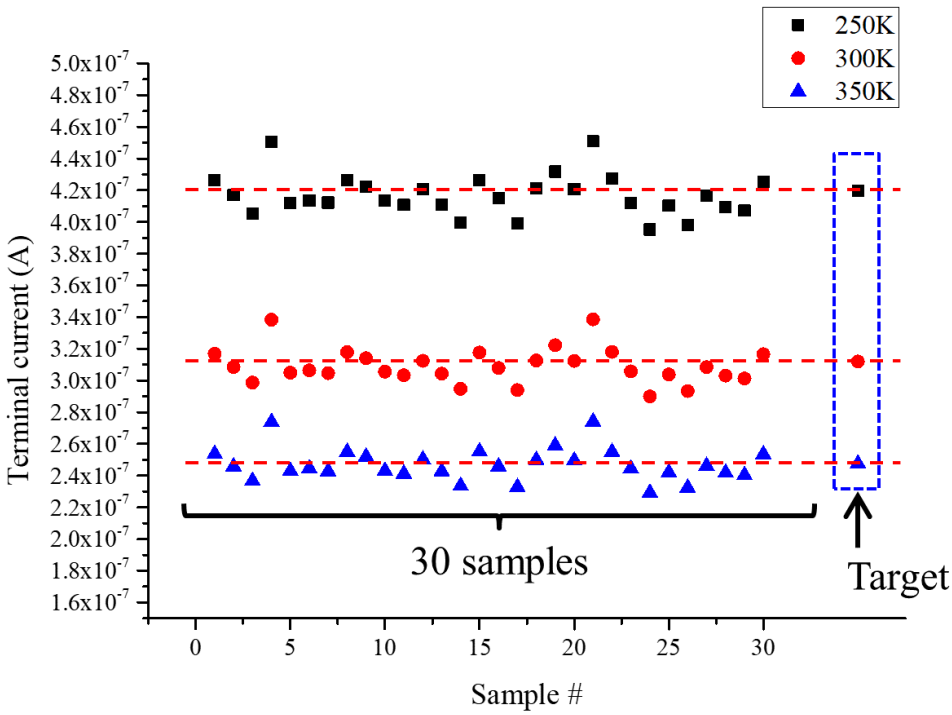

Fig. 3.9. Comparison between the 'target' currents (red dot lines) and the currents of the 30 discrete samples (solid dots).

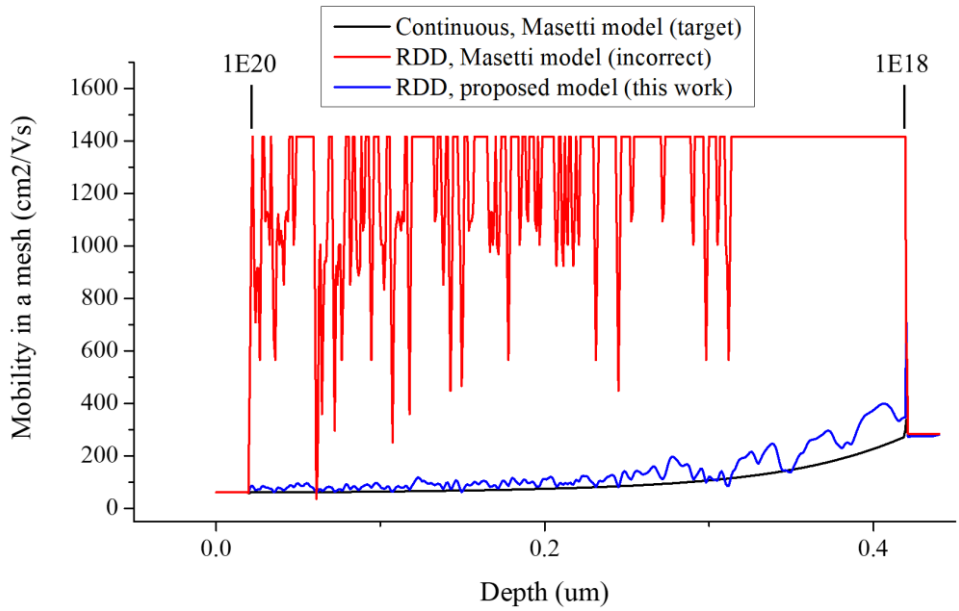

Fig. 3.10. Mobility values in meshes along the longitudinal center of the simulation structures of Fig. 3.8. In the RDD sample, the proposed model (blue line) provides the proper mobility profile in comparison to the target case (black line), whereas the Masetti model (red line) fails.

Chapter 4. Discussion

4.1. Physical Explanation of the Terms in the Model

In the first term in μ_{dop} (15) with $B(T)$ and β in Table 3.1, it is interesting to notice that $B(T)$ has the linear dependency to the inverse of the temperature, and the value of β is extracted to be about 1/3 even though the proposed model has been extracted to fit the mobility data in the bulk doping concentrations. The 1/3-order dependency on the field is analogous to terms in the universal mobility curves [20]. In the universal mobility curve of the inversion layer, the mobility limited by the phonon scattering μ_{ph} depends on 0.3-order of the effective field which includes the quantum mechanical picture of the inversion layer [23,27]. Since the proposed model also includes the quantum mechanics by means of the DG method, the extracted value of $\beta \approx 1/3$ in the model may be coincident or may have the similar physical origin with the surface inversion layer. In the next section, the proposed model will be applied to the inversion layer of the MOSFET devices.

Now, let us discuss the second term in μ_{dop} (15) with $C(T)$ and γ in Table 3.1. With $C(T)$ having the exponential dependency to the inverse of the temperature and γ being approximately the value of 3/2, the average terminal currents could fit the target currents with the error rate below 1% for wide range of the doping concentration and temperature simultaneously. The second term may be considered to come from some scattering mechanism which only occurs far from the discrete impurities. From Fig. 4.1 showing the contribution of each scattering term in (14) with the mobility field, the second term in the proposed model is dominant for the

regime of the low mobility field. So, it possibly means this term describes the long-ranged Coulomb interaction and its temperature dependency. The theoretical derivation should be investigated by the future study.

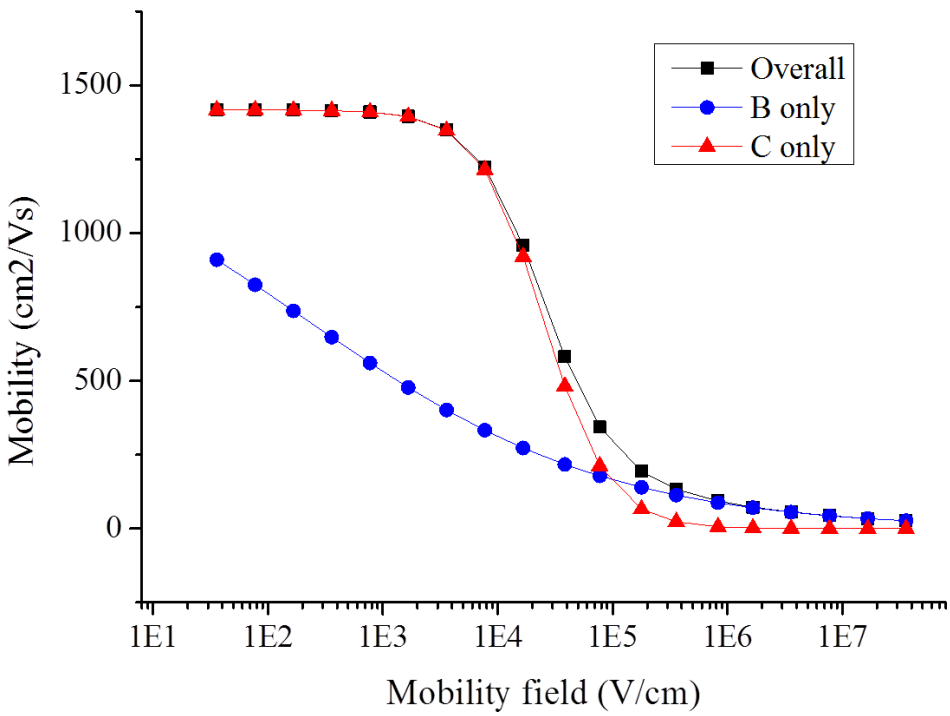

Fig. 4.1. Contribution of each term in the mobility formula for the temperature of 300 K. $B(T)$ term governs the high E_{mob} region, and $C(T)$ term dominates in the low E_{mob} region.

4.2. Possible Extension to the Inversion Layer Mobility

From the simulation of the I-V/C-V characteristics of the conventional MOSFET using the proposed mobility model, the effective field and the effective mobility are plotted following the same procedure in [20]. To evaluate the effective mobility, the low frequency (1 kHz) C-V characteristics for the inversion electron density qN_s and the low drain voltage (10 mV) I-V characteristics for the transconductance g_d are necessary, respectively, as follows,

$$qN_s\left(V_g\right)=\int_{-\infty}^{V_g} C_{gc}\left(V_g\right)dV_g \tag{18}$$

$$\mu_{eff}=\frac{L}{W}\frac{g_d\left(V_g\right)}{qN_s\left(V_g\right)} \tag{19}$$

Furthermore, to calculate the effective field of (6), the depletion charge density qN_{dpl} should be also evaluated, as follows,

$$\phi_B=\frac{k_BT}{q}\ln\left(\frac{N_{sub}}{n_i}\right) \tag{20}$$

$$N_{dpl}=\sqrt{\frac{4\varepsilon_{Si}\phi_BN_{sub}}{q}} \tag{21}$$

To plot the universal mobility curves, two sets of the mobility models are adopted; (i) the conventional empirical models (Masetti and Lombardi), and (ii) the proposed model which originally aim to describe the bulk mobility near the

discrete dopants. It should be noted the device under consideration is intrinsic MOSFET and the mobility degradation in the inversion layer may be considered due to the Coulomb scattering with the charge in the gate by way of the effective field at the surface.

As shown in Fig. 4.2, two cases of the mobility model result in the parallel universal mobility curves, which are related to the similar 1/3-order dependency in

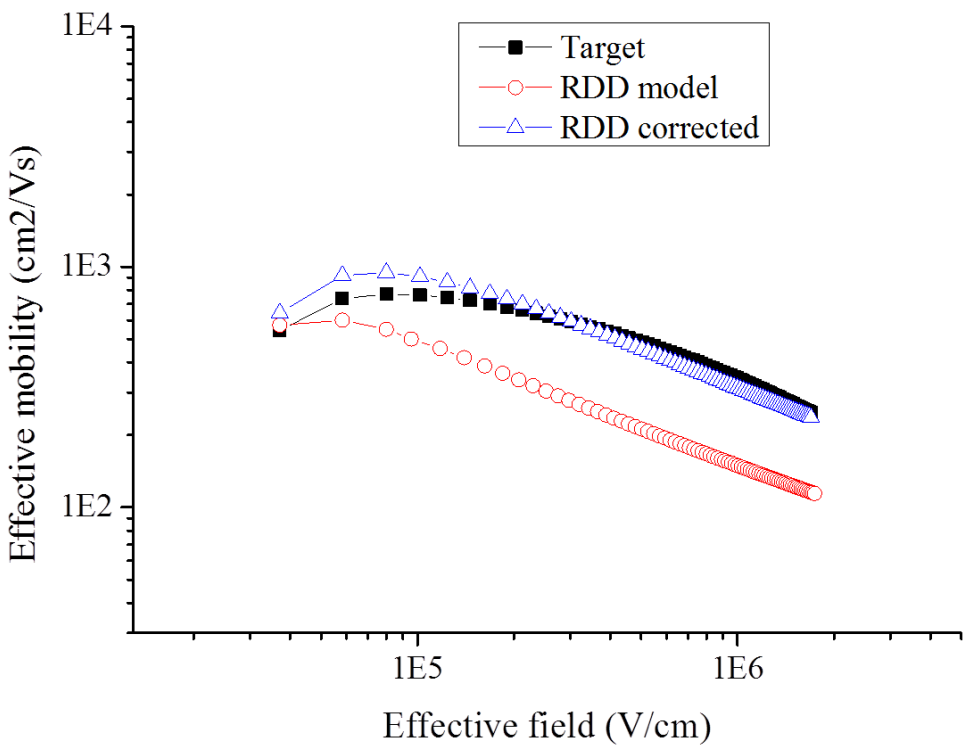

Fig. 4.2. Universal mobility curves evaluated from TCAD simulations with (i) the conventional mobility model (black solid), (ii) the proposed mobility model for bulk resistor (red open), and (iii) the modified model (6) with l_{crit} of 3 um (blue open), respectively.

the proposed mobility model and the Lombardi's surface mobility model. Also, the proposed model predicts lower mobility values for the range of the surface effective field considered in this work.

For completeness of the mobility modeling, the formula (14) may be modified as follows,

$$\frac{1}{\mu(\boldsymbol{r})} = \frac{1}{\mu_{\max}} + \frac{\exp(-z / l_{\text{crit}})}{\mu_{\text{dop}}} \tag{22}$$

where z is the normal distance from the dielectric-substrate surface. With the appropriate parameter l_{crit} value, the model with (22) follows the surface mobility value pretty well, as shown in Fig. 4.2. The term added in (22) is borrowed from the Lombardi model in (8) and (11). By this term, the affecting range of the mobility model is limited at the vicinity of the silicon-dielectric interface. The distance z is set to zero in the S/D regions because of the lack of the gate interfaces, so the modified model becomes the original bulk mobility formula (14). In this way, it is possible for the modified version of the proposed model (22), to apply to both the Masetti and Lombardi model for the simulation of the MOSFET devices including the RDD.

In the supplemental simulation, the exponential term in (22) is applied separately in $B(T)$ and $C(T)$ terms with the separate l_{crit} values, respectively, as follows:

$$\frac{1}{\mu(\boldsymbol{r})} = \frac{1}{\mu_{\max}} + \frac{1}{\frac{B(T)}{E_{\mathrm{mob}}^{\beta}}\exp(z / l_{\mathrm{crit1}}) + \frac{C(T)}{E_{\mathrm{mob}}^{\gamma}}\exp(z / l_{\mathrm{crit2}})} \tag{23}$$

If two scattering mechanisms are different, the affecting distance l_{crit} may be separated, as in (23). Since the $C(T)$ term has been assumed to be originated from the long-range interaction in the previous section, $l_{\mathrm{crit2}} > l_{\mathrm{crit1}}$ was expected. However, in the supplemental simulation, the resultant effective mobility μ_{eff} is mainly affected by the value of l_{crit1}, not l_{crit2}, since $B(T)$ governs the range of the effective field (also the mobility field) over 10^5 V/cm, as previously shown in Fig 4.1. If the additional simulations are conducted with relatively lower range of the effective field, the value of l_{crit2} can be determined, which should be exploited in the future study.

4.3. Consideration of the hot electron effects with the RDD

In this thesis, the proposed mobility model of (14) has been established under the low drain bias (20 mV) in order to describe the bulk mobility with the RDD. However, if the drain voltage increases, the velocity saturation is inevitably occurred by the hot electron effects [26]. The conventional empirical mobility model for the hot electron effects are known as the Caughey-Thomas model of (12). Since the ON-current condition of most of the semiconductor devices is under the high drain bias, the RDD effect under the high drain voltage should also be exploited properly, as well as the bulk mobility.

However, if the conventional Caughey-Thomas model is applied in the RDD

structures, the resultant terminal currents are diminished as shown in Fig 4.3, even though the bulk mobility had been corrected by the proposed mobility model in this thesis. The reason of decreasing currents can be analyzed by the fluctuation of the local electric fields. If the formula of the Caughey-Thomas model is recalled:

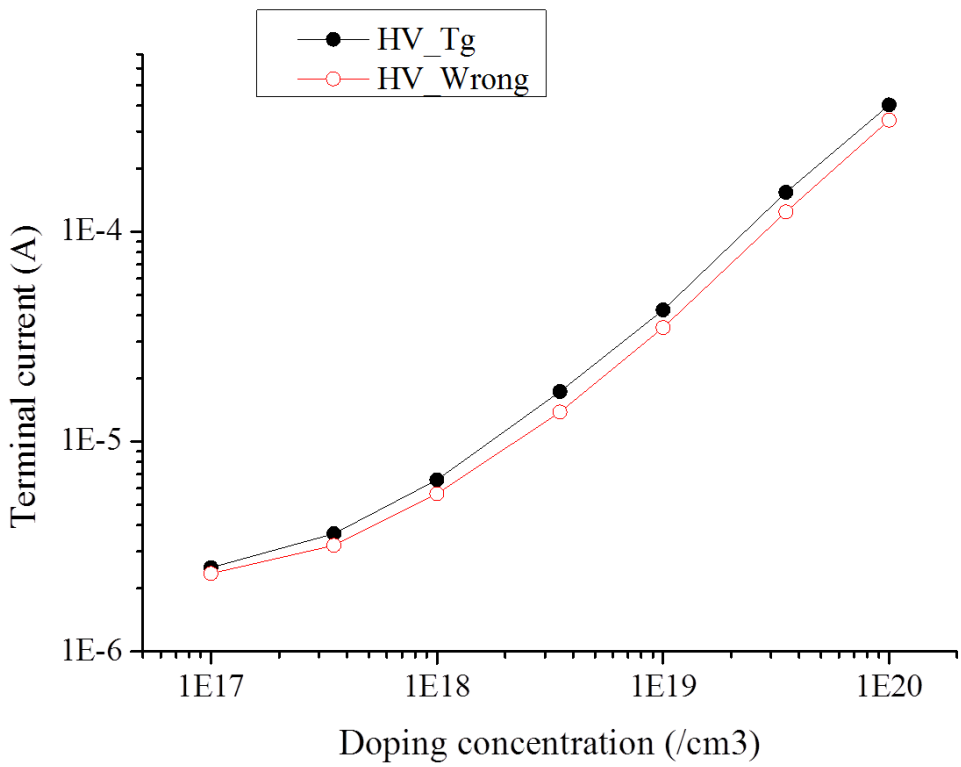

Fig. 4.3. Terminal currents as a function of the doping concentration under the high drain bias (3 V). The 'target' currents are evaluated by the conventional mobility models (Masetti and Caughey-Thomas). The average currents of the discrete samples are evaluated by the proposed mobility model for the bulk mobility, but the Caughey-Thomas model is applied blindly.

$$\mu = \frac{\mu_{\text{low}}}{\left(1+\left(\frac{\mu_{\text{low}}E}{v_{\text{sat}}}\right)^{\beta}\right)^{1/\beta}} \tag{12}$$

it is reasonable that the hot electron is occurred by the local electric field E, not by the quantum field E_{mob}. In the vicinity of the RDD, the profile of the local field fluctuates extremely because of the abrupt gradient of the doping concentration. As a result, the fluctuation of the local field leads to overestimate the degradation of the mobility values by the velocity saturation model.

In the previous work, the value of β in the Caughey-Thomas model is modified until the average terminal current of the RDD samples reproduces the 'target' current [19]. The procedure of the modifying the parameter may be practical, but not based on the physical scattering mechanism. In order to consider the physical scattering, the proposed mobility model in this thesis may be complemented by a term which is governed by the local electric field, as follows:

$$\frac{1}{\mu(\boldsymbol{r})} = \frac{1}{\mu_{\max}} + \frac{1}{\frac{B(T)}{E_{\text{mob}}^{\beta}} + \frac{C(T)}{E_{\text{mob}}^{\gamma}}} + \frac{1}{\frac{F(T)}{E_{\parallel}^{\delta}}} \tag{24}$$

where $E_{\parallel}(\boldsymbol{r})$ is the local electric field of the direction aligned to the local current density, $E_{\parallel}(\boldsymbol{r}) = \boldsymbol{E}(\boldsymbol{r}) \cdot \boldsymbol{J}(\boldsymbol{r})$. Determining the additional parameter $F(T)$ and δ should be conducted in order to complete the mobility model for the RDD, which may be left as a future study.

Chapter 5. Conclusion

In this thesis, the ‘effective field dependent’ mobility model has been proposed for the simulation including the random discrete dopants. Through the definition of the ‘mobility field’ which is consistent to the effective field in the MOS surfaces, the mobility formula is established with the consideration of the scattering mechanisms. Since the proposed model has been verified for wide range of temperatures and nonuniform doping profiles, this model can be generally applied for estimating the mobility and the resultant current of any circumstances with the random discrete dopants. Furthermore, the bulk model has been extended to the inversion layer mobility, so the proposed model can be extended to modeling the characteristics of the MOSFET devices including the random discrete dopants in the source/drain region.

As possible future works, the following research topic can be dealt with;

(i) The incorporation of the velocity saturation model into the proposed mobility model will be necessary. In the thesis, the target mobility model is limited to the Masetti model in the low bias (20 mV) condition in order to neglect the velocity saturation effect. The effect will emerge when the drain bias reaches in the practical level up to 0.5 V. In this situation, the electric field in the vicinity of the discrete dopants should be considered, so the mobility field defined in this thesis may not be appropriate to describe the mobility in each mesh. The additional term with the local electric field may have to be complemented in the proposed model. The electron temperature evaluated from the hydrodynamic transport instead of the drift-diffusion may be considered.

(ii) The range of the lattice temperature should be widened in order to apply the proposed mobility model more generally. At a glance of the simulation in the very low temperature of 77 K, the dependency of the coefficients (linear and exponential) has failed to maintain the general formulae suggested in the thesis. To become applicable in the wider range of the temperature, the formulae for the coefficients should be modified, and the low temperature physics model should also be considered.

(iii) The universal curve by the proposed model applied in the traditional MOSFET devices blindly has to be exploited because the curve predicts lower mobility values than the conventional mobility models. This possibly means that the scattering by the gate charges induced by the gate voltage may be weaker than the effect from the discrete dopants as the fixed charges. It can be considered that the gate charges should overcome the thickness of the dielectric layer, while the individual dopants are able to affect to the mobile carrier in the closer distances.

(iv) The careful study for the modification to apply in the surface mobility has to be conducted. Even though the proposed model has been modified in the last section of this thesis, the universal mobility curve has still deviation from the empirical result by the conventional mobility models, such as Masetti, Lombardi, and Canali. In the low and high regime of the effective field, the universal curve has different aspects respectively, so there is the crossing point between two curves. This possibly indicates that the physical scattering mechanism may be different between the low and high region of the effective field.

Bibliography

[1] R. W. Keyes, “The effect of randomness in the distribution of impurity atoms on FET thresholds,” *Appl. Phys.*, vol. 8, no. 3, pp. 251–259, 1975.

[2] H.-S. Wong and Y. Taur, “Three-dimensional ‘atomistic’ simulation of discrete random dopant distribution effects in sub-0.1 μm MOSFET’s,” in *IEDM Tech. Dig.*, 1993, pp. 705–708.

[3] T. Mizuno, J. Okamura, and A. Toriumi, “Experimental study of threshold voltage fluctuation due to statistical variation of channel dopant number in MOSFET’s,” *IEEE Trans. Electron Devices*, vol. 41, no. 11, pp. 2216–2221, 1994.

[4] X. Tang, V. K. De, and J. D. Meindl, “Intrinsic MOSFET parameter fluctuations due to random dopant placement,” *IEEE Trans. VLSI Technol.*, vol. 5, pp. 369–376, Dec. 1997.

[5] A. Asenov, “Random dopant induced threshold voltage lowering and fluctuations in sub-0.1 μm MOSFET’s: A 3-D ‘atomistic’ simulation study,” *IEEE Trans. Electron Devices*, vol. 45, no. 12, pp. 2505–2513, Dec. 1998.

[6] P. A. Stolk, F. P. Widdershoven, and D. B. M. Klaassen, “Modeling statistical dopant fluctuations in MOS transistors,” *IEEE Trans. Electron Devices*, vol. 45, no. 9, pp. 1960–1971, Sept. 1998.

[7] D. J. Frank, Y. Taur, M. Ieong, and H.-S. P. Wong, “Monte Carlo modeling of threshold variation due to dopant fluctuations,” in *Symp. VLSI Technol. Dig.*, 1999, pp. 169–170.

[8] N. Sano, K. Matsuzawa, M. Mukai, and N. Nakayama, “On discrete random dopant modeling in drift-diffusion simulations: physical meaning of

‘atomistic’ dopants,” *Microelectron. Reliab.*, vol. 42, no. 2, pp. 189–199, Feb. 2002.

[9] G. Slavcheva, J. H. Davies, A. R. Brown, and A. Asenov, “Potential fluctuations in metal-oxide-semiconductor field-effect transistors generated by random impurities in the depletion layer,” *J. Appl. Phys.*, vol. 91, no. 7, pp. 4326–4334, Apr. 2002.

[10] G. Roy, A. R. Brown, F. Adamu-Lema, S. Roy, and A. Asenov, “Simulation study of individual and combined sources of intrinsic parameter fluctuations in conventional nano-MOSFETs,” *IEEE Trans. Electron Devices*, vol. 53, no. 12, pp. 3063–3070, Dec. 2006.

[11] M.-H. Chiang, J.-N. Lin, K. Kim, and C.-T. Chuang, “Random dopant fluctuation in limited-width FinFET technologies,” *IEEE Trans. Electron Devices*, vol. 54, no. 8, pp. 2055–2060, Jul. 2007.

[12] D. Reid, C. Millar, G. Roy, S. Roy, and A. Asenov, “Analysis of threshold voltage distribution due to random dopants: A 100 000-sample 3-D simulation study,” *IEEE Trans. Electron Devices*, vol. 56, no. 10, pp. 2255–2263, Oct. 2009.

[13] X. Wang *et al.*, “Statistical threshold-voltage variability in scaled decananometer bulk HKMG MOSFETs: A full-scale 3-D simulation scaling study,” *IEEE Trans. Electron Devices*, vol. 58, no. 8, pp. 2293–2301, Aug. 2011.

[14] J. M. Park *et al.*, “20 nm DRAM: A new beginning of another revolution,” in *IEDM Tech. Dig.*, 2015, pp. 676–679.

[15] T. Shinada, S. Okamoto, T. Kobayashi, and I. Ohdomari, “Enhancing semiconductor device performance using ordered dopant arrays,” *Nature*, vol. 437, no. 7062, pp. 1128–1131, Oct. 2005.

[16] A. Asenov, G. Slavcheva, A. R. Brown, J. H. Davies, and S. Saini, “Increase in the random dopant induced threshold fluctuations and lowering in sub-100 nm MOSFETs due to quantum effects: a 3-D density-gradient simulation study,” *IEEE Trans. Electron Devices*, vol. 48, no. 4, pp. 722–729, Apr. 2001.

[17] S. M. Amoroso *et al.*, “Modeling carrier mobility in nano-MOSFETs in the presence of discrete trapped charges: accuracy and issues,” *IEEE Trans. Electron Devices*, vol. 61, no. 5, pp. 1292–1298, May 2014.

[18] S. M. Amoroso, F. Adamu-Lema, A. R. Brown, and A. Asenov, “A mobility correction approach for overcoming artifacts in atomistic drift-diffusion simulation of nano-MOSFETs,” *IEEE Trans. Electron Devices*, vol. 62, no. 6, pp. 2056–2060, Jun. 2015.

[19] H. Yu, D. Kim, S. Rhee, S, Choi, and Y. J. Park, “A mobility model for random discrete dopants and application to the current drivability of DRAM cell,” *IEEE Trans. Electron Devices*, vol. 64, no. 10, pp. 4246–4251, Oct. 2017.

[20] S. Takagi, A. Toriumi, M. Iwase, and H. Tango, “On the universality of inversion layer mobility in Si MOSFET’s: Part I–effects of substrate impurity concentration,” *IEEE Trans. Electron Devices*, vol. 41, no. 12, pp. 2357–2362, Dec. 1994.

[21] G. Masetti, M. Severi, and S. Solmi, “Modeling of carrier mobility against carrier concentration in arsenic-, phosphorus-, and boron-doped silicon,” *IEEE Trans. Electron Devices*, vol. 30, no. 7, pp. 764–769, Jul. 1983.

[22] *Sentaurus TCAD Tools*, Synopsys, Mountain View, CA, USA, 2015.

[23] K. Lee, J.-S. Choi, S.-P. Sim, and C.-K. Kim, "Physical understanding of low-field carrier mobility in silicon MOSFET inversion layer," *IEEE Trans. Electron Devices*, vol. 38, no. 8, pp. 1905–1912, Aug. 1991.

[24] M. G. Ancona and G. J. Iafrate, "Quantum correction to the equation of state of an electron gas in a semiconductor," *Phys. Rev. B*, vol. 39, no. 13, pp. 9536–9540, May 1989.

[25] C. Lombardi, S. Manzini, A. Saporito, and M. Vanzi, "A physically based mobility model for numerical simulation of nonplanar devices," *IEEE Trans. Computer-Aided Design*, vol. 7, no. 11, pp. 1164–1171, Nov. 1988.

[26] D. M. Caughey and R. E. Thomas, "Carrier mobilities in silicon empirically related to doping and field," *Proc. IEEE*, vol. 55, no. 12, pp. 2192–2193, Dec. 1967.

[27] S. A. Schwarz and S. E. Russek, "Semi-empirical equations for electron velocity in silicon: Part II–MOS inversion layer," *IEEE Trans. Electron Devices*, vol. 30, no. 12, pp. 1634–1639, Dec. 1983.

국 문 초 록

본 연구에서는 랜덤 불연속 도펀트를 포함한 시뮬레이션에 적용할 수 있는 유효 전기장 의존 이동도 모델을 수립하였다. 랜덤 불연속 도펀트를 포함한 구조를 시뮬레이션 하는 경우, 정전기적 모델과 이동도 모델이 모두 수정되어야 한다. 정전기적 모델의 경우, MOS 구조 표면에서 제안된 밀도 경사 방법(density gradient method)이 개별 도펀트 주변의 양자역학적 효과를 잘 모사하지만, 이동도 모델의 경우 그 중요성에도 불구하고 아직 완벽한 모델이 제안된 바 없다.

Masetti 모델과 같은 기존의 불순물 농도 의존 이동도 모델은, 소자의 크기가 불순물 농도의 변화 범위에 비해 상대적으로 큰 경우 잘 맞는 모델로서 기능해 왔다. 그러나, 시뮬레이션에 랜덤 불연속 도펀트를 도입하는 경우, 기존의 Masetti 모델은 부정확하게 높은 전류 결과를 주게 된다. Masetti 모델의 불순물 농도 의존성으로 인해, 극소수의 극도로 높은 불순물 농도를 가진 점(개별 도펀트를 모사)의 이동도는 매우 낮게 계산되지만, 이를 제외한 나머지 모든 영역은 고유(intrinsic) 농도로서 이동도가 최대값으로 계산되며, 이로 인해 전체 전류가 높아지는 문제가 있다. 이를 위해, 랜덤 불연속 도펀트 시뮬레이션에 적용 가능한 새로운 이동도 모델이 필요하다.

먼저, 기존의 Takagi *et al.*에 의해 제안된 유효 전기장의 정의로부터, 새로운 유효 '이동도 전기장' 을 각 점에 대해 정의하였다. 이 이동도

전기장은 기존의 유효 전기장과 물리적인 일관성을 유지하도록 정의되었는데, 이는 MOS 시뮬레이션을 통해 확인되었다. 그리고 이 이동도 전기장으로부터 각 점의 이동도 공식을 수립하였으며, 목표 전류가 나오도록 하는 파라미터를 찾아내었다. 이 새로운 이동도 모델과 파라미터를 통해서, 여러 불순물 농도와 온도의 조합에서 목표 전류가 1% 이내의 오차로 잘 재현되는 것을 확인하였다.

또한, 결정된 파라미터 중, 계수들은 각각 온도의 역수에 선형 비례하거나 지수 비례하는 특징이 있고, 이동도 전기장에 대한 지수들은 1/3과 3/2에 가까운 값을 가지도록 추출되었다. 온도의 역수에 선형 비례하면서 전기장의 1/3승 의존도를 갖는 항은 Takagi *et al.*의 보편 이동도 곡선이나, 기존의 표면 이동도 열화 모델인 Lombardi 모델과 같은 양자역학을 고려한 여러 모델에도 찾아볼 수 있는데, 이를 통해 개별 도펀트 주변에서의 산란 현상이 MOS 표면에서와 동일한 물리적 원인을 가짐을 추론할 수 있다.

주요어: 랜덤 불연속 도펀트, TCAD 시뮬레이션, 이동도 모델, 유효 전기장, 전기장 의존 이동도

학번: 2016-20870